Geophysical Research Letters

Supporting Information for

Asynchronous Poleward Migration of the Atlantic Subtropical Gyres over the past 22,000 years

Tainã M. L. Pinho[1*]; Hu Yang[2,1*]; Gerrit Lohmann[1,3]; Rodrigo C. Portilho-Ramos[3]; Cristiano M. Chiessi[4]; Andre Bahr[5]; Dirk Nürnberg[6]; Janne Repschläger[7]; Xiaoxu Shi[1]; Ralf Tiedemann[1]; Stefan Mulitza[3]

[1]Alfred Wegener Institute for Polar and Marine Research, Bremerhaven, Germany.
[2]Southern Marine Science and Engineering Guangdong Laboratory, Zhuhai, China.
[3] MARUM—Center for Marine Environmental Sciences, University of Bremen, Bremen, Germany.
[4] School of Arts, Sciences and Humanities, University of São Paulo, São Paulo, Brazil.
[5] Institute of Earth Sciences, Heidelberg University, Heidelberg, Germany.
[6] GEOMAR Helmholtz Centre for Ocean Research Kiel, Kiel, Germany.
[7] Department of Climate Geochemistry, Max Planck Institute for Chemistry, Hahn-Meitner-Weg 1, 55128 Mainz, Germany

*Correspondence to taina.pinho@awi.de & yanghu@sml-zhuhai.cn

Contents of this file

Supporting text

Marine sediment cores

Marine sediment cores distributed along the North and South Atlantic were assembled (Fig. 1 and Tab. S1). The selection criteria were based on the geographic location and temporal resolution of the cores covering the last deglacial interval. Our dataset, comprising the abundance of *Globorotatia truncatulinoides* records, is predominantly available on the World Data Center PANGAEA data repository. In total, we utilized 577 data points derived from the relative

abundance of *G. truncatulinoides* across nine marine sediment cores (Tab. S1). An outlier value of 14.9% at 3.44 ka. in core GIK15612-2 was excluded from the analysis. Further details regarding the age models and counting methodology of *G. truncatulinoides* are available be in the original publications (Tab. S1).

Morphology and genotypes of *Globorotalia truncatulinoides* morphospecies in the Atlantic Ocean

Globorotalia truncatulinoides is a planktonic foraminifer comprising a complex of four to five species, as revealed by genetic and morphometric analyses (Quillévéré et al., 2013; Ujiié et al., 2010; de Vargas et al., 2001). The Atlantic basin, particularly the South Atlantic, exhibits diverse morphological and genetic variants of the *G. truncatulinoides* complex (Darling & Wade, 2008; de Vargas et al., 2001). While distinguishing specific genotypes in downcore records remains challenging, the analysis of coiling directions (dextral and sinistral morphotypes) serves as a more practical approach in studying faunal compositions in geological records. Although these species demonstrate glacial-interglacial habitat changes associated with variations in shape and size (Renaud & Schmidt, 2003), their coiling directions have remained remarkably stable in the South Atlantic since the last glacial period. The dextral morphotype predominantly occurs at the northern boundary of the South Atlantic subtropical gyre (nSASG), while the sinistral variant dominates the southern boundary (sSASG) since the last glacial period, a distribution pattern further confirmed by Pinho et al. (2021).

The ForCens database, the most comprehensive up-to-date resource on modern planktic foraminifera distribution (Siccha & Kucera, 2017a, 2017b), provides variations in the meridional distribution of dextral and sinistral morphotypes of *G. truncatulinoides*. Specifically, the sinistral morphotype is more prevalent in the subtropical (mid-latitude) domains of both the Atlantic subtropical gyres, while the dextral morphotype is more commonly found in tropical (lower latitude) regions and the eastern portion of the North Atlantic subtropical gyre (Siccha & Kucera, 2017a, 2017b). It is noteworthy that the most accurate representation of physical oceanographic conditions for the subtropical gyre circulation is achieved when both coiling directions are considered together (Fig. 1a and b). Consequently, both coiling directions effectively represent the upper water column stratification conditions associated with subtropical gyres (Fig. 1). As also previously shown in Fig. 1 of Pinho et al. (2021), the abundance of both morphotypes (sinistral + dextral) of *G. truncatulinoides* follows more accurately the thermocline structure of the Atlantic subtropical gyres. This relationship confirms that *G. truncatulinoides* is indeed an ideal proxy for upper water stratification (e.g., Schiebel & Hemleben, 2017).

Importantly, no significant differences in the abundance of sinistral and dextral coiling directions are observed across all records in our study, which spans the past 22 ka. At the northern boundary of the North Atlantic Subtropical Gyre (nNASG), the dextral morphotype accounts for 77% of the total. This contribution increases to 85.6% at the southern boundary of the NASG (sNASG). At nSASG, the dextral morphotype further rises to 94.8%. Conversely, at the sSASG, 97.5% of the total is attributed to the sinistral morphotype. The monomodal biogeographical domains of sinistral and dextral morphotypes of *G. truncatulinoides* follow the modern and typical regional-specific morphotype domains as compiled by Siccha & Kucera (2017a) (2017b) for the North and South Atlantic basins. In these biogeographical domains there are different genotypes of *G. truncatulinoides* that are likely influenced by distinct upper water stratification, productivity, and temperature conditions (Darling & Wade, 2008; Renaud & Schmidt, 2003; de Vargas et al., 2001). Given that the primary modern distribution pattern of the complex of *G. truncatulinoides* species is associated with subtropical gyres (Fig. 1a-c), changes in upper water stratification are likely assumed to be the main limiting factor controlling their abundance. Moreover, the relatively brief 22,000-year timespan precludes any evolutionary processes (cladogenesis) that might have altered the geographical distribution of *G. truncatulinoides* species through changes in colonization environments.

While *G. truncatulinoides* distribution at boundaries of the Atlantic subtropical gyres is primarily controlled by changes in upper water stratification caused by meridional gyre displacement, genetic variations within the species may also play a role (Ujiié et al., 2010; de Vargas et al., 2001). Thus, increases and decreases in the abundance of *G. truncatulinoides* in response to meridional migrations of the Atlantic subtropical gyres may be accompanied by specific changes in their species by habitat tracking process (Renaud & Schmidt, 2003), particularly at the sSASG. For instance, at the sSASG the *G. truncatulinoides* genotype Type III and Type IV are basically controlled by changes in temperature (Renaud & Schmidt, 2003). According to our interpretation, during the glacial period the sSASG shifted northward, which is aligned with the SST cooling, hence possibly favoring the genotype IV. Yet, the relative abundance of *G. truncatulinoides* species clearly decreases during the glacial period, which indicates that this genotype Type IV was not successful. This further confirms that increases and decreases in *G. truncatulinoides* is sensitive to changes in the sSASG rather than other parameters. Since there is only right-coiled morphotype at the nSASG, we assume that the *G. truncatulinoides* species reflects the genotype Type II (Renaud & Schmidt, 2003; de Vargas et al., 2001), which likely dominates the North Atlantic subtropical gyre boundaries as well (De Vargas et al. 2001; Renauld and Schmidt, 2003). Regardless of the cryptic species and morphotypes of *G. truncatulinoides* present in our studied records, changes in upper water column stratification remain the critical limiting factor for their proliferation at the Atlantic subtropical gyre boundaries. This approach, however, is only effective

100 in regions experiencing abrupt changes in upper water stratification due to meridional migration
101 of the Atlantic subtropical gyres, specifically at their northern and southern boundaries as
102 presented here.

103

104 **Modern distribution of *Globorotalia truncatulinoides***

105 We utilized the modern spatial distribution of planktonic foraminifera *Globorotalia*
106 *truncatulinoides* in the Atlantic Ocean sediments, as documented in the ForCenS database (Siccha
107 & Kucera, 2017a, 2017b). The remarkable overlap of its spatial distribution with upper water
108 column structure, circulation and physico-chemical properties suggest that conditions within the
109 subtropical gyres are favorable for *G. truncatulinoides*. Therefore, this species can be used to
110 track meridional position of the Atlantic subtropical gyres (Kucera et al., 2005; Lohmann &
111 Schweitzer, 1990; Mulitza et al., 1997; Siccha & Kucera, 2017a, 2017b) (Fig 1a and b, see also
112 Fig. 1 of Pinho et al., 2021). *Globorotalia truncatulinoides* exhibits higher abundances within the
113 gyre due to the deeper thermocline (weaker stratification) and is virtually absent immediately to
114 the north and south of the gyre domain where the thermocline is shallow. Therefore, this species
115 is a recorder of subsurface conditions.

116 In Siccha & Kucera (2017a, 2017b), foraminifera were picked from the > 150 μm size fraction of
117 sample splits containing around 300 specimens (Siccha & Kucera, 2017a, 2017b), the same
118 method applied in records used here. Further details on the ages of modern surface sediments can
119 be found in Siccha & Kucera (2017a). Modern foraminiferal data used here are available from the
120 World Data Center PANGAEA (ForCenS) (https://doi.pangaea.de/10.1594/PANGAEA.873570)
121 (Siccha & Kucera, 2017b).

122 **2.3 Change-point analysis on long-term *Globorotalia truncatulinoides* records**

123 We applied change-point analysis to identify the points in time at which the abundances of
124 *Globorotalia truncatulinoides* increase or decrease, indicating long-term poleward shifts. The
125 change-point detection was based on two different methods, which are the Binary Segmentation
126 (Binseg) (Truong et al., 2020) and Hidden Markov Models (HMM, Rabiner, 1989). The analysis
127 were performed in Pandas library and hmmlearn package both in Python. To identify the long-
128 term we smoothed the records with larger variability using a 5 point running average smoothing
129 for the following cores: M35003-4, M125-95-3, TNO57-21, and MD07-3076Q. The smoothing
130 of the data preserve the main patterns in the original data as shown in Figure 2. Therefore, the
131 change-point detection for these cores was based on the smoothed data.

132 Both the Binseg and HMM methods yielded similar change-points as summarized in the table S2,
133 with few exceptions in cores M125-95-3 and MD07-3076Q (Tab. S2). Slight differences in the

change-point detection in these cores can be attributed to different baseline values chose in Binseg and HMM methods. We took the change-point mean from both methods. We determined the "point of no return" in Fig. 2 based on this assessment. Visual inspection clearly confirms the onset of long-term poleward trends (Fig. 2).

We observe a longer delayed response for the poleward shift between cores MD95-2041 and GIK15612-2/ SU92-03 (North Atlantic subtropical gyre northern boundary (nNASG)) in comparison to that between cores TNO57-21 and MD07-3076Q (South Atlantic subtropical gyre southern boundary (sSASG)). This difference is due to the distance where these cores are located, i.e., 5-6° latitude-long distance at the nNASG and 3° latitude-long distance at the sSASG. Note that the rate of poleward shift at the nNASG is 0.83°/kyr and sSASG is 0.84°/kyr, hence showing a great similarity.

Table S1.

Downcore records of the relative abundance of *Globorotalia truncatulinoides* in the North and South Atlantic subtropical gyres

Core ID	Region	Latitude (˚N)	Longitude (˚E)	Water depth (m)	Period covered (kyr)	Analyzed core section Interval (m)	Number of samples	References (records)
GIK15612-2	NE-North Atlantic	44.36	-26.54	3050	22 – 2.3	0.0075 – 0.685	29	(Kiefer, 1998)
SU92-03	NE- North Atlantic	43.19	-10.11	3005	22 – 0.9	0.025 – 1.325	30	(Salgueiro et al., 2010)
GEOFAR KF16	Central North Atlantic	37.99	-31.12	3050	11.34 – 0.52	0.025 – 1.965	134	(Repschläger et al., 2015, 2023)
MD08-3180	Central North Atlantic	37.99	-31.13	3064	15.45 – 11.25	1.505 – 3.805	107	(Repschläger et al., 2015, 2023)
MD95-2041	NE- North Atlantic	37.83	-9.51	1123	22 – 0	0.05 – 3.965	43	(Voelker, 2010)
M35003-4	SW- North Atlantic	12.09	-61.24	1299	22 – 0	0 –3.550	72	(Hüls & Zahn, 2000)
M125-95-3	NW-South Atlantic	-10.94	-36.20	1897	22 – 0	0 – 2.180	44	(Pinho et al., 2021)
TNO57-21	SE-South Atlantic	-41.10	7.80	4981	22 – 10.3	1.000 – 2.3000	64	(Barker et al., 2009)

MD07-3076Q	Central South Atlantic	-44.15	-14.28	3770	22 – 1.3	0.105 – 1.565	54	(Gottschalk et al., 2015)

146

147

148

Table S2.

Change-point detection of the relative abundance of *Globorotalia truncatulinoides* in the North and South Atlantic

Core ID	Region	Binary Segmentation	Hidden Markov Models	References (records)
GIK15612-2	NE-North Atlantic	8.89 ka	8.89 ka	(Kiefer, 1998)
SU92-03	NE- North Atlantic	7.5 ka	7 ka	(Salgueiro et al., 2010)
MD95-2041	NE- North Atlantic	14.5 ka	14.5 ka	(Voelker, 2010)
M35003-4	SW- North Atlantic	7.5 ka	7.3 ka	(Hüls & Zahn, 2000)
M125-95-3	NW-South Atlantic	10.6 ka	8.2 ka	(Pinho et al., 2021)
TNO57-21	SE-South Atlantic	16 ka	15.95 ka	(Barker et al., 2009)
MD07-3076Q	Central South Atlantic	11.4 ka	13.31 ka	(Gottschalk et al., 2015)

149

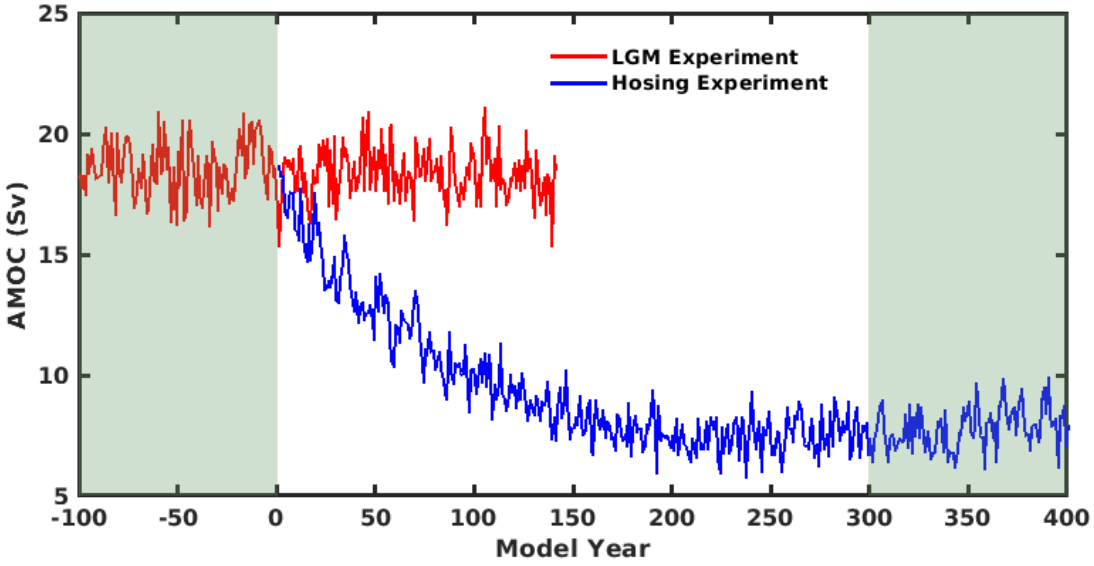

Figure S1. Strength of the Atlantic Meridional Overturning Circulation (AMOC) in the Last Glacial Maximum control experiment (red line) and 0.1 Sv freshwater hosing experiment (blue line). After applying the freshwater perturbation over the North Atlantic Ocean, the AMOC strength reduced from ~18 Sv to ~8 Sv within a few hundred years. The climate state during the 300-400th model years of the hosing experiment was compared to that of the control experiment, during the -100-0 model years (initial and final periods highlighted by green patches).

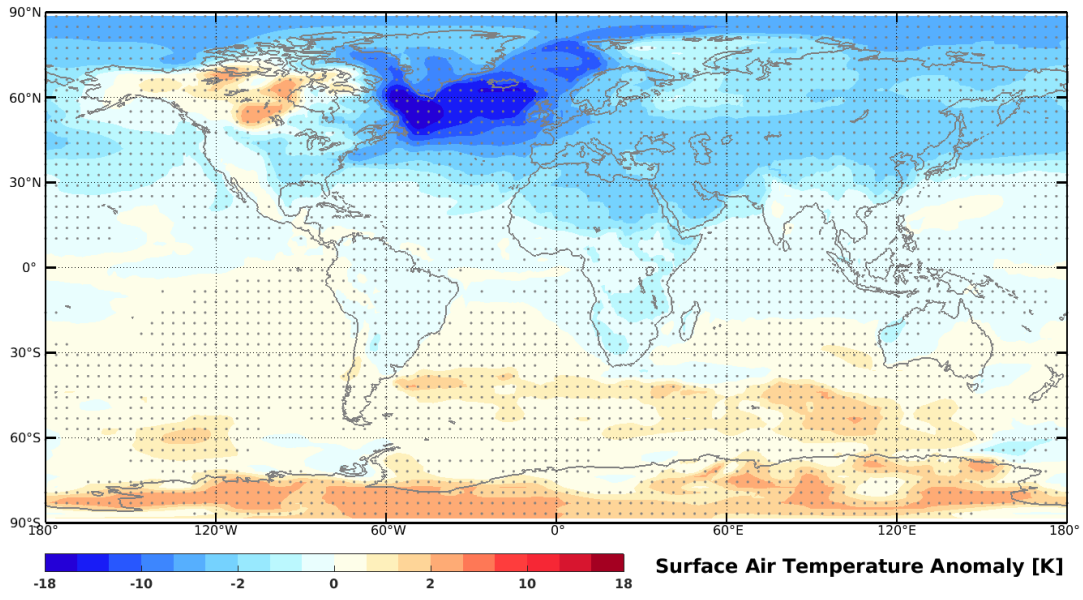

Figure S2. Surface air temperature anomalies during the millennial cold period (e.g., HS1 and YD) depicted by the 300-400th model years of the hosing experiment with respect to the -100-0 model years of the LGM control experiment performed by the AW1-ESM. Stippling denotes areas where anomalies are statistically significant (two-tailed Student's t-test). A bipolar seesaw is observed with a cooling signal over the Northern Hemisphere and a warming signal over the Southern Hemisphere.

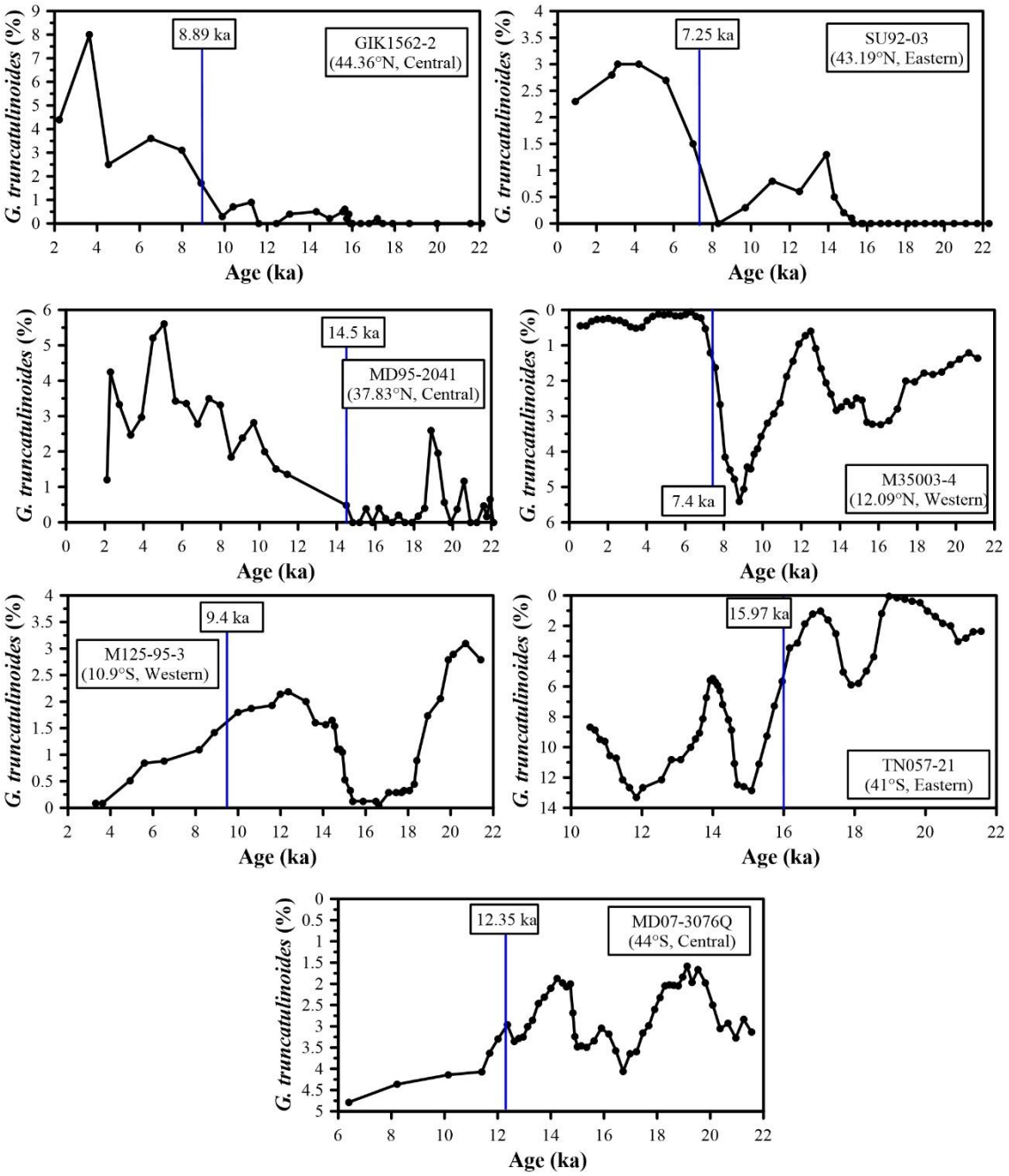

Figure S3. Change-point detection on record of *Globorotalia truncatulinoides* at the North and South Atlantic subtropical relative to its poleward shift. To better determine the change-points, we use smoothed the data from cores M35003-4, M125-95-3, TNO57-21, and MD07-3076Q using a 5pts-running average smoothing. The change-points shown are based on both Binary Segmentation (Binseg) (Truong et al., 2020) and Hidden Markov Models (HMM, Rabiner, 1989).